

Why hematite is red: Correlation of optical absorption intensities and magnetic moments of Fe³⁺ minerals

GEORGE R. ROSSMAN

Division of Geological and Planetary Sciences, California Institute of Technology,
Pasadena, California 91125, U.S.A.

Abstract—Structures with Fe³⁺ shared through oxo- or hydroxyl-groups have antiferromagnetic interactions. Such interactions result in enhanced intensity of the Fe³⁺ optical absorption bands which in some systems can be as great as a factor of 100 compared to isolated, octahedrally coordinated Fe³⁺ ions. A comparison is presented between the intensity of the lowest energy crystal-field band of Fe³⁺ minerals and their magnetic moments which demonstrates the dependence of optical absorption intensity and antiferromagnetic interactions in the host phase. Hematite, which is usually responsible for the red color of geological materials, owes its intense color to these magnetic interactions.

INTRODUCTION

OXIDIZED IRON (Fe³⁺) is associated with the red color which is commonly observed in many soils, sedimentary rocks and weathering products (BLODGETT *et al.*, 1993). In these materials, Fe³⁺, primarily in the form of finely disseminated hematite (Fe₂O₃), is an intense pigment. The prevalence of hematite as a red pigment in geological materials leads to the common association of red color with oxidized iron in general.

On the other hand, a variety of other Fe³⁺ minerals and chemical compounds are pale colored. Many examples exist of pale colored Fe³⁺ minerals including light greenish-yellow silicates such as andradite garnet, and lavender phosphates and sulfates such as strengite and coquimbite. A problem has been to reconcile the intense color of hematite and related hydrous iron oxides with the pale color of many other Fe³⁺ minerals and compounds.

ROSSMAN (1975, 1976a,b) noted that the intensity of color per unit of Fe³⁺ ions in iron sulfates increases dramatically when the iron ions are joined through shared oxide and hydroxide ions (shared edges or vertices of coordination polyhedra). He observed that such systems are antiferromagnetic and suggested that, in these systems, the intensity of color was related to the extent of magnetic interaction. Furthermore, ferric sulfate systems joined through shared oxide ions often show much greater magnetic interaction and stronger color than those joined through hydroxide ions.

SHERMAN (1985) and SHERMAN and WAITE (1985) discussed the results of molecular orbital

calculations on clusters with Fe³⁺-O and Fe³⁺-OH units. They found that the Fe³⁺-OH bond was more ionic and had a smaller spin-polarization than the Fe³⁺-O bond. This gave rise to much weaker magnetic exchange (superexchange) between hydroxyl-bridged Fe³⁺ cations compared to oxo-bridged Fe³⁺ cations. In addition to the effects discussed by Sherman on the internal magnetic hyperfine fields observed in the Mössbauer spectra, superexchange interactions produce the major intensifications of the Fe³⁺ ligand field transitions in the optical spectra (ROSSMAN, 1975, 1976a,b).

This paper presents empirical correlations between the intensities of optical absorption bands and the magnetic susceptibility of Fe³⁺ minerals. These observations provide experimental support for the concepts developed by SHERMAN (1985). As part of these correlations, the special case of the color of hematite and other hydrous iron oxides is considered.

EXPERIMENTAL

Magnetic and optical data were taken from the literature or were determined by the methods described in ROSSMAN (1975). Both new and reviewed data are presented in Table 1.

RESULTS AND DISCUSSION

The optical absorption spectrum of Fe³⁺ in an octahedral site isolated from other Fe³⁺ octahedra consists of two broad bands at lower energies (labeled ⁴T_{1g} and ⁴T_{2g} in order of increasing energy) and a pair of bands, often overlapping near 440 nm, labeled (⁴A_{1g}, ⁴E_g). The light not absorbed by these bands determines the color of Fe³⁺ minerals.

Table 1. Spectral and magnetic data

Sample	Formula	$\lambda(^4T_{1g})$	ϵ	$\lambda(^4A_{1g}, ^4E_g)$	ϵ	μ
Regular Octahedra						
1 andradite	$Ca_3Fe_2(SiO_4)_3$	854	0.08	440	1.5	-
Distorted Octahedra						
2 coquimbite	$Fe_2(SO_4)_3 \cdot 9H_2O$	778	0.18	427	2.0	5.87
3 phosposiderite	$FePO_4 \cdot 2H_2O$	746	0.34	423	6.5	-
Dimer						
4 magnesiocopiapite	$MgFe_4(SO_4)_6(OH)_2 \cdot 20H_2O$	864	1.7	430	36	4.70
Chains						
5 butlerite	$Fe(SO_4)(OH) \cdot 2H_2O$	920	2.4	424	33	3.8
6 parabutlerite	$Fe(SO_4)(OH) \cdot 2H_2O$	912	2.5	426	28	3.3
7 stewartite	$MnFe_2(PO_4)_2(OH)_2 \cdot 8H_2O$	880	2.3	428	55	-
8 fibroferrite	$Fe(SO_4)(OH) \cdot 5H_2O$	840	1.9	423	11	3.72
9 botryogen	$MgFe(SO_4)_2(OH) \cdot 7H_2O$	939	3.4	432	96	3.97
Clusters						
10 metavoltine	$K_2Na_6FeFe_6(SO_4)_{12}O_2 \cdot 18H_2O$	855	5.5	464	66	3.42
11 amarantite	$Fe(SO_4)(OH) \cdot 3H_2O$	866	12.7	442	90	2.53
12 leucophosphate	$KFe_2(PO_4)_2(OH) \cdot 2H_2O$	800	0.78	441	8.4	5.13
13 pharmocosiderite	$KFe_4(AsO_4)_3(OH)_4 \cdot 7H_2O$	820	0.5	446	19	4.71
Extended Structures						
14 hematite	Fe_2O_3	855	15.3	-	-	2.06
15 goethite	$FeO(OH)$	915	7.0	-	-	3.23
16 lepidocrocite	$FeO(OH)$	918	13.5	-	-	3.01
17 bernalite	$Fe(OH)_3$	885	0.12	431	1.95	-

Wavelengths of absorption bands (λ) in nm; molar absorption coefficients (ϵ) in $l/mol \cdot cm^{-1}$; effective magnetic moments (μ) in Bohr magnetons at approximately 295°C.

Sources of data: 1 (MAO and BELL, 1974); 2-9 (ROSSMAN, 1975, 1976a,b); 10 (previously unpublished); 11,12 (ROSSMAN, 1976b); 13 (previously unpublished); 14 (BAILEY, 1960; HOFER *et al.*, 1946); 15,16 (MAO *et al.* 1974, HOFER *et al.*, 1946); 17 (McCAMMON *et al.*, 1995)

Andradite garnet, $Ca_3Fe_2(SiO_4)_3$, is a mineral containing such isolated octahedral Fe^{3+} sites. The general features of the spectrum of andradite (Fig. 1) are typical for Fe^{3+} in octahedral coordination in a variety of silicate, sulfate and phosphate minerals. The two broad bands at longer wavelengths ($^4T_{1g}$ and $^4T_{2g}$) have low intensity and do not produce strong colors in a thickness of a few millimeters and the more intense, sharp band near 440 nm is so far in the violet that it contributes little to the color of the mineral.

In hematite, all Fe^{3+} sites are adjacent to other Fe^{3+} sites. In Fig. 1 the hematite spectrum (in the

(0001) plane) is compared to the spectrum of andradite. The spectra are normalized for density and iron concentration such that they are presented for equal amounts of Fe^{3+} in the sample path. From this comparison, it can be seen that hematite has a much greater absorption intensity than andradite. The intense, deep red color of hematite is determined by the narrow transmission window near 750 nm.

The absolute intensity of the bands is measured in terms of the molar absorption coefficient, ϵ , defined by absorbance = $\epsilon (l/mol \times cm^{-1}) \times path (cm) \times concentration (moles/liter)$. The ϵ value for

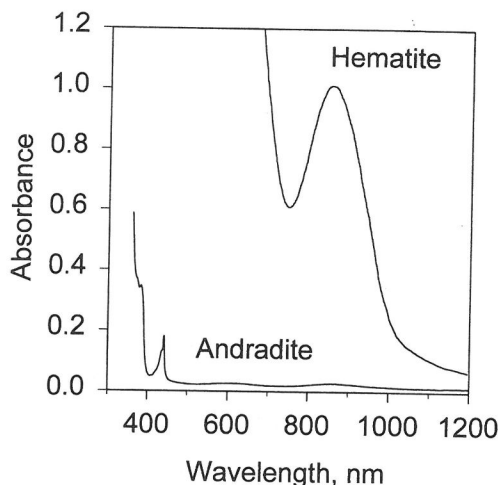


FIG. 1. Comparison of the optical absorption spectra of hematite and andradite garnet. The spectra have been normalized for density and Fe-concentration so that they are presented for identical amounts of Fe in the sample path.

hematite is 15.3 in the 850 nm region compared to 0.08 for andradite. This increase of intensity of absorption by over two orders of magnitude coupled with increased intensity of the higher energy bands is responsible for the intense color of hematite.

A general observation which follows from these studies is that intense color and high absorption band intensity is associated with minerals which have chains, clusters or extended networks of Fe^{3+} cations. This observation is reinforced by Fig. 2 which illustrates that the intensity of the ${}^4\text{T}_{1g}$ band is generally much greater for various clusterings of Fe^{3+} cations than for Fe^{3+} in isolated, symmetrical or moderately distorted octahedra. Similar behavior is observed for the often sharp (${}^4\text{A}_{1g}$, ${}^4\text{E}_g$) band near 440 nm (Table 1). In the case of anisotropic absorption, the data are presented for the polarization direction with the greatest intensity. Comparable intensification is not observed for the ${}^4\text{T}_{2g}$ band in many of these systems, so this band is not further considered. The apparent exceptions to this generalization which involve clusters and extended structures based on hydroxyl units as the shared ion are rationalized on the basis of the magnetic interactions in such units.

Magnetic interactions usually accompany clustering or polymerization of the Fe^{3+} cations.

Thus it is necessary to consider the correlation between intensity of absorption and the strength of the magnetic interaction. For many minerals, the intensity of the (${}^4\text{A}_{1g}$, ${}^4\text{E}_g$) band is often difficult to measure due to overlap with the tail of intense absorption bands in the ultraviolet. In nearly all cases, the ${}^4\text{T}_{1g}$ band near 800 nm is unaffected by this tail. Its intensity is therefore more amenable to quantification. The strength of the magnetic interaction can be measured through the magnetic moment, derived from measurements of the mineral's bulk magnetic susceptibility. The effective magnetic moment of Fe^{3+} ions isolated from anti-ferromagnetic interactions is about 5.9 Bohr magnetons. Strong antiferromagnetic interactions decrease this value to about 2.0 in the case of pairs of Fe^{3+} bridged by a nearly linear oxo-bridge (SCHUGAR *et al.*, 1972). The intensity of the ${}^4\text{T}_{1g}$ band increases markedly as the magnetic moment per Fe^{3+} decreases due to magnetic exchange interactions (Fig. 3). Although the concept is well established that absorption band intensification is related to magnetic interactions, Fig. 3 provides a quantitative demonstration of this relationship and illustrates that there is some variation from a smooth trend, undoubtedly caused by variations in the structural details of the interacting Fe^{3+} sites.

A visible manifestation of the importance of these magnetic interactions is the intensity of color of the host phases. If Fe^{3+} in the host mineral is free of magnetic interactions the mineral is usually pale yellow-green (typically silicates) or pale lavender (phosphates and sulfates). The reds and browns usually associated with Fe^{3+} are observed

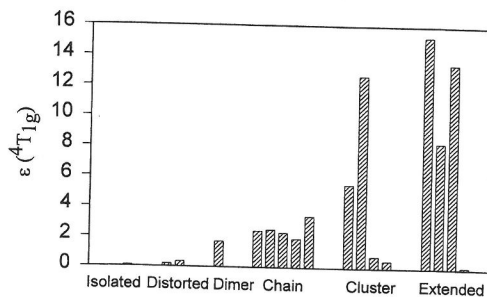


FIG. 2. Bar graph illustrating the range of molar absorption coefficients for the ${}^4\text{T}_{1g}$ band in the 750 - 950 nm range in a variety of minerals with Fe^{3+} in different distortions and types of polyhedral linkages. In all cases, Fe^{3+} absorption intensity is much greater when the Fe^{3+} ions are magnetically coupled through shared polyhedra.

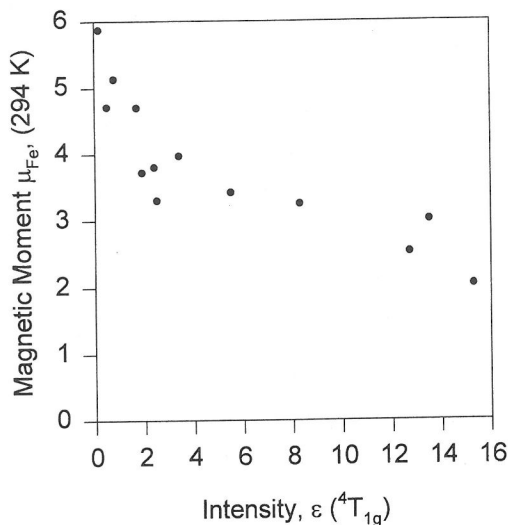


FIG. 3. Comparison of the effective room temperature magnetic moment per Fe^{3+} and the intensity of the first ligand field band (${}^4T_{1g}$). Absorption intensity is greatest for minerals with strong antiferromagnetic coupling between adjacent Fe^{3+} cations.

only in minerals with strong magnetic interactions due to extensive polyhedral sharing.

The importance of O-linkages between Fe^{3+} rather than OH-linkages in providing the pathway for absorption band enhancement has previously been noted (ROSSMAN, 1976b) in the tetrameric clusters of amaranthite (deep red, oxo-bridged cluster) and leucophosphate (pale amber, hydroxyl-bridged cluster). The importance of oxo-linkages is further demonstrated by the contrast between hematite, Fe_2O_3 , which has oxo-linkages and a deep red color with $\epsilon_{855\text{ nm}} = 15.3$, and bernalite, $Fe(OH)_3$, which has hydroxyl-linkages (BIRCH *et al.*, 1993), a green color, and $\epsilon_{885\text{ nm}} = 0.12$ calculated from the data presented in MCCAMMON *et al.* (1995).

The relationship between magnetic interactions and enhanced intensity of light absorption can be simply explained using crystal field theory by considering the electronic states of isolated Fe^{3+} ions and magnetically coupled ions. In isolated octahedrally coordinated Fe^{3+} , all electronic transitions require a change in the electronic spin state of the ion. As such, to first order, they are forbidden by the quantum mechanical laws which govern such transitions and will happen, in practice, with low probability. Consequently, the intensity of light absorption will be low as will be the corresponding intensity of color.

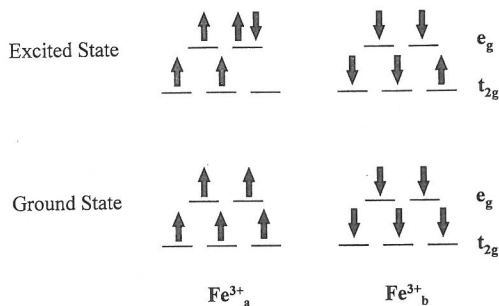


FIG. 4. Orbital energy diagram for a pair of adjacent magnetically coupled Fe^{3+} ions before (bottom) and after (top) an electronic transition illustrating the coupled electronic promotion and spin orientation changes which results in no net electronic spin change for the coupled system.

In a magnetically coupled system, the electrons in adjacent Fe^{3+} ions interact to circumvent the spin selection rules by acting collectively as a system. Fig. 4 illustrates the ground state of a pair of Fe^{3+} ions with strong magnetic interaction. When an electronic excitation (promotion of an electron to an orbital of higher energy) occurs on Fe^{3+}_a , the promoted electron must change its spin state when it pairs with the higher energy electron. If simultaneously an electron on the adjacent Fe^{3+}_b changes its spin state without a corresponding promotion to a higher energy orbital, the net spin state of the system remains unchanged. Thus, the simultaneous electronic and magnetic state transition of the paired system does not represent a spin-forbidden process. The transition is spin-allowed; the intensity of light absorption will be much higher, as will be the corresponding intensity of color. This concept, developed for a pair of interacting Fe^{3+} ions, is also applicable to more extended interacting clusters and networks of Fe^{3+} ions such as hematite.

Acknowledgments—Support for optical spectroscopy of minerals has been provided by the White Rose Foundation and the National Science Foundation (USA). Contribution number 5624 of the Division of Geological and Planetary Sciences.

REFERENCES

- BAILEY P. C. (1960) Absorption and reflectivity measurements on some rare earth iron garnets and $\alpha\text{-Fe}_2\text{O}_3$. *J. Appl. Phys.* **31**, 39s-40s.
- BIRCH W. D., PRING A., RELLER A. and SCHMALLE H. W. (1993) Bernalite, $Fe(OH)_3$, a new mineral from

- Broken Hill, New South Wales—description and structure. *Amer. Mineral.* **78**, 827–834.
- BLODGETT R. H., CRABAUGH J. P. and MCBRIDE E. F. (1993) The color of red beds; a geologic perspective. In: *Soil Color*, Soil Sci. Soc. Amer., Madison, WI, USA, Spec. Pub. **31**, pp. 127–159.
- HOFER L. J. E., PEEBLES W. C. and DIETER W. E. (1946) X-ray diffraction and magnetic studies of unreduced ferric oxide Fischer-Tropsch catalysts. *J. Amer. Chem. Soc.* **68**, 1953–1956.
- MAO H. K. and BELL P. M. (1974) Crystal-field effects of ferric iron in goethite and lepidocrocite: band assignment and geochemical applications at high pressure. *Carnegie Inst. Wash. Year Book* **73**, 502–506.
- MCCAMMON C. A., PRING A., KEPPLER H. and SHARP T. (1995) A study of bernalite, $\text{Fe}(\text{OH})_3$, using Mössbauer spectroscopy, optical spectroscopy and transmission electron microscopy. *Phys. Chem. Mineral.* **22**, 11–20.
- ROSSMAN G. R. (1975) Spectroscopic and magnetic studies of ferric iron hydroxy sulfates: intensification of color in ferric iron clusters bridged by a single hydroxide ion. *Amer. Mineral.* **60**, 698–704.
- ROSSMAN G. R. (1976a) Spectroscopic and magnetic studies of ferric iron hydroxy sulfates: the series $\text{Fe}(\text{OH})\text{SO}_4 \times n\text{H}_2\text{O}$ and the jarosite. *Amer. Mineral.* **61**, 398–404.
- ROSSMAN G. R. (1976b) The optical spectroscopic comparison of ferric iron tetrameric clusters in amarantite and leucophosphite. *Amer. Mineral.* **61**, 933–938.
- SCHUGAR H. J., ROSSMAN G. R., BARRACLOUGH C. G. and GRAY H. B. (1972) Electronic structure of oxo-bridged iron(III) dimers. *J. Amer. Chem. Soc.* **94**, 2683–2690.
- SHERMAN D. M. (1985) The electronic structures of Fe^{3+} coordination sites in iron oxides; Applications to spectra, bonding and magnetism. *Phys. Chem. Mineral.* **12**, 161–175.
- SHERMAN D. M. and WAITE T. D. (1985) Electronic spectra of Fe^{3+} oxides and oxide hydroxides in the near IR to near UV. *Amer. Mineral.* **70**, 1262–1269.

